Elevated subsarcolemmal Ca^{2+} in *mdx* mouse skeletal muscle fibers detected with Ca^{2+}-activated K^+ channels

Nora Mallouk, Vincent Jacquemond, and Bruno Allard*

Laboratoire de Physiologie des Eléments Excitables, Unité Mixte de Recherche, Centre National de la Recherche Scientifique 5578, Université Claude Bernard Lyon I, 43 Boulevard du 11 Novembre 1918, 69622 Villeurbanne Cedex, France

Edited by William A. Catterall, University of Washington School of Medicine, Seattle, WA, and approved February 24, 2000 (received for review November 1, 1999)

Duchenne muscular dystrophy results from the lack of dystrophin, a cytoskeletal protein associated with the inner surface membrane, in skeletal muscle. The cellular mechanisms responsible for the progressive skeletal muscle degeneration that characterizes the disease are still debated. One hypothesis suggests that the resting sarcolemmal permeability for Ca^{2+} is increased in dystrophic muscle, leading to Ca^{2+} accumulation in the cytosol and eventually to protein degradation. However, more recently, this hypothesis was challenged seriously by several groups that did not find any significant increase in the global intracellular Ca^{2+} in muscle from *mdx* mice, an animal model of the human disease. In the present study, using plasma membrane Ca^{2+}-activated K^+ channels as subsarcolemmal Ca^{2+} probe, we tested the possibility of a Ca^{2+} accumulation at the restricted subsarcolemmal level in *mdx* skeletal muscle fibers. Using the cell-attached configuration of the patch-clamp technique, we demonstrated that the voltage threshold for activation of high conductance Ca^{2+}-activated K^+ channels is significantly lower in *mdx* than in control muscle, suggesting a higher subsarcolemmal [Ca^{2+}]. In inside-out patches, we showed that this shift in the voltage threshold for high conductance Ca^{2+}-activated K^+ channel activation could correspond to a $\approx$3-fold increase in the subsarcolemmal Ca^{2+} concentration in *mdx* muscle. These data favor the hypothesis according to which an increased calcium entry is associated with the absence of dystrophin in *mdx* skeletal muscle, leading to Ca^{2+} overload at the subsarcolemmal level.

Duchenne muscular dystrophy is characterized by the absence of the protein dystrophin in skeletal muscles (1). This protein is associated with a complex of sarcolemmal glycoproteins and is thought to link the cytoskeleton to the extracellular matrix (e.g., refs. 2 and 3). The absence of dystrophin leads to progressive degeneration in muscles from patients with Duchenne muscular dystrophy as well as in muscles from the dystrophic *mdx* mouse, an animal model that has been and is still used widely to study the pathophysiology of the human disease (4). The cellular mechanisms responsible for muscle necrosis in patients with Duchenne muscular dystrophy and *mdx* mice are still debated. It has been suggested that the absence of dystrophin could induce an increase of sarcolemmal Ca^{2+} influx via abnormally functioning mechanosensitive channels in myotubes and adult muscle fibers from *mdx* mice (5, 6) or nonselective leak cation channels in Duchenne muscular dystrophy and *mdx* myotubes as well as in *mdx* muscle fibers (7–9). This increased sarcolemmal Ca^{2+} entry was thought to give rise to an elevation of cytosolic free calcium concentration, activation of proteases, and eventually to muscle necrosis (10). Nevertheless, more recently, an increase in the global intracellular [Ca^{2+}] has not been found by several groups working on *mdx* muscle fibers under similar experimental conditions (11–15), casting doubt on the existence of a perturbation in global Ca^{2+} homeostasis in dystrophic muscle (16).

With respect to the increased sarcolemmal Ca^{2+} entry described in dystrophic muscle, one possibility could be that a high calcium concentration stays confined within a restricted submembranous space as postulated by Turner *et al.* (8). Classic Ca^{2+} fluorescence methods are thought not to offer the required resolution to estimate the [Ca^{2+}] in the immediate vicinity of the membrane. Ca^{2+} indicators containing a hydrophobic tail that attaches them to the membrane also have been used (17) but may be not specifically restricted to the plasma membrane (18). A different approach that has been used to probe the subsarcolemmal [Ca^{2+}] was to use endogenous plasmalemmal Ca^{2+} sensors. In this respect, the activity of Ca^{2+}-activated K^+ channels has been used extensively in smooth muscle to measure submembranous [Ca^{2+}] (e.g., ref. 19). High conductance Ca^{2+}-activated K^+ channels (K_{Ca}) are present in the sarcolemma of skeletal muscle (for reviews see refs. 20–24). These channels also have been described in *mdx* mouse skeletal muscles (25). We thus used these skeletal muscle K^+ channels to investigate the possible existence of a Ca^{2+} overload at the subsarcolemmal level in *mdx* muscle fibers.

In this paper, using the inside-out configuration of the patch-clamp technique, we first compared the Ca^{2+}- and voltage-dependence properties of K_{Ca} channels in control and *mdx* muscle fibers. Then, using the cell-attached configuration, we measured the voltage threshold for K_{Ca} channel activation (E_{th}) and built partial voltage activation curves in control and *mdx* muscle fibers as an index of subsarcolemmal [Ca^{2+}]. Finally, using the inside-out configuration, we estimated the subsarcolemmal [Ca^{2+}] corresponding to these thresholds.

Materials and Methods

Isolation of Skeletal Muscle Fibers. Wild-type (C57BL/10ScSn) and *mdx* (C57BL/10*mdx*) mice aged 3–5 weeks (period corresponding to the peak of degeneration in *mdx* muscle; ref. 26) were killed by cervical dislocation. Isolated skeletal muscle cells were obtained from the flexor digitorum brevis, and interosseal muscles by a classical enzymatic dissociation process; muscles were incubated for 1 h at 37°C in Tyrode's solution containing collagenase (2 mg/ml, Sigma, Type 1). After enzyme treatment, muscles were rinsed with Tyrode's solution and stored in Tyrode's solution at 4°C until use. Intact skeletal muscle fibers were separated from the muscle mass by gently triturating the muscle with a plastic Pasteur pipette. The absence of significant immu-

This paper was submitted directly (Track II) to the PNAS office.

Abbreviations: K_{Ca}, high conductance Ca^{2+}-activated K^+ channels; E_{th}, voltage threshold for K_{Ca} channel activation.

*To whom reprint requests should be addressed. E-mail: bruno.allard@physio.univ-lyon1.fr.

The publication costs of this article were defrayed in part by page charge payment. This article must therefore be hereby marked "*advertisement*" in accordance with 18 U.S.C. §1734 solely to indicate this fact.

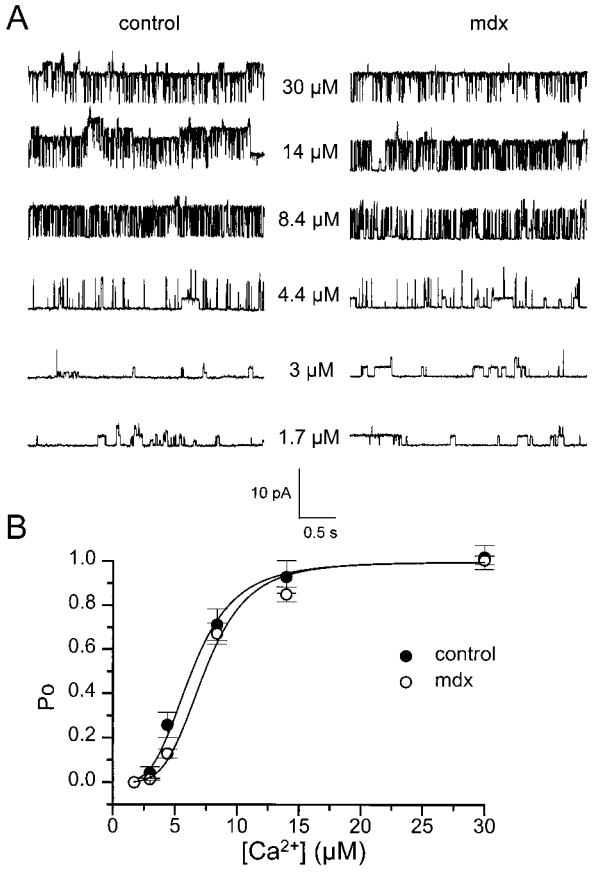

Fig. 1. Comparison of Ca^{2+} sensitivity of K_{Ca} channels in inside-out patches from control and *mdx* muscle fibers. (*A*) Segments of single K_{Ca} channel currents recorded in the presence of increasing intracellular free [Ca^{2+}] indicated next to each current trace. The membrane potential was held at 0 mV. (*B*) Relationships between open probability and intracellular free [Ca^{2+}] in control (●; $n = 14$) and *mdx* (○; $n = 19$) patches. In each patch, values of P_o were normalized to the value obtained in the presence of 2.5 mM intracellular Ca^{2+}. The curves were fitted by using a Hill equation with $n = 3.6$ and $K = 6.3$ μM in control and $n = 4.2$ and $K = 7.4$ μM in *mdx* patches, respectively (see text).

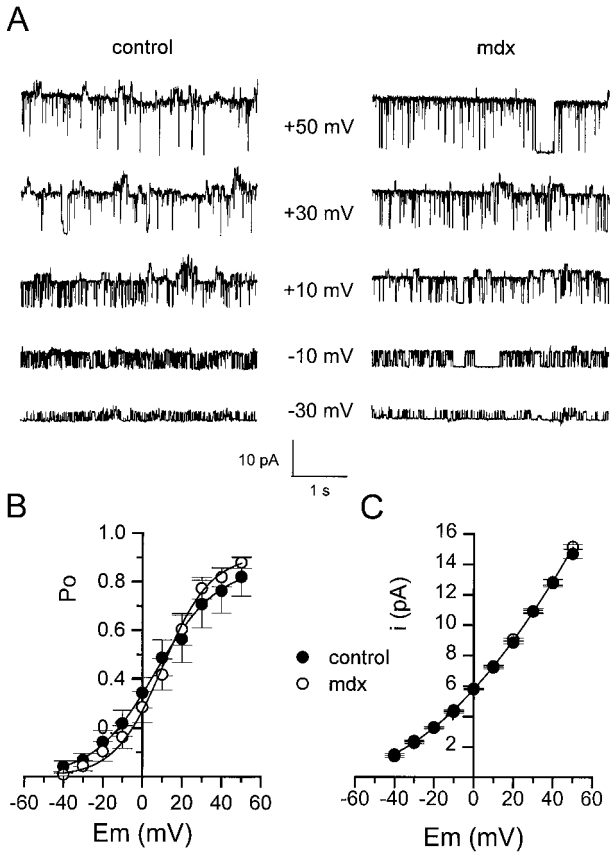

Fig. 2. Comparison of voltage sensitivity of K_{Ca} channels in inside-out patches from control and *mdx* muscle fibers. (*A*) Segments of single K_{Ca} channel currents recorded in the presence of 4.4 μM intracellular free [Ca^{2+}] at different membrane potentials indicated next to each current trace. (*B*) Relationships between open probability and membrane potential in control (●) and *mdx* (○) patches. In each patch, values of P_o were normalized to the value obtained at 0 mV in the presence of 2.5 mM intracellular Ca^{2+}. The curves were fitted with a Boltzmann equation with $V_{1/2} = 6.8$ mV and $k = 15.6$ mV in control and $V_{1/2} = 10.4$ mV and $k = 12.1$ mV in *mdx* patches, respectively (see text). (*C*) Current-voltage relationships of K_{Ca} channels in control (●; $n = 14$) and *mdx*(○; $n = 17$) patches. The curve was drawn by eye.

nofluorescent labeling of dystrophin was checked in *mdx* muscle fibers as described in a preceding study performed in the laboratory (27). All experiments were carried out at room temperature (20–23°C).

Electrophysiology. Single-channel currents were recorded from cell-attached or inside-out membrane patches by using a patch-clamp amplifier (model RK 400; Biologic, Claix, France). Currents flowing into the pipette were considered to be positive. Command voltage pulse generation and acquisition were done by using the BIOPATCH software (Biologic) driving an A/D, D/A converter (Lab Master DMA board, Scientific Solutions, Solon, OH). Currents were analyzed with BIOPATCH software. For Fig. 1 and 2, channel open-state probability (P_o) was determined from the average current (I) as $P_o = I/Ni$, where i is the single channel current and N is the number of channels in the patch. I was measured after filtering at 300 Hz and sampling at 1 kHz over 3-s recording periods. Single-channel current amplitudes were determined with amplitude histograms. For Fig. 3, E_{th} was evaluated after filtering at 300 Hz and sampling at 1 kHz over 3-s recording periods by determining the membrane potential at which an opening of a channel with a conductance greater than 70 pS (the conductance of K_{Ca} channels at 0 mV in the presence of 5 mM K^+ at the external face of the membrane) was detected. For Fig. 4, P_o was determined by measuring the proportion of time channels with a conductance greater than 70 pS spent in the open state, divided by N, after filtering at 300 Hz and sampling at 1 kHz over 10-s recording periods. N was determined in inside-out patches by exposing the cytoplasmic face to a 2.5 mM Ca^{2+}-containing internal solution. Capacitive transients were subtracted from current traces.

The pipette resistance was checked regularly before seal establishment. It ranged from 3 to 4.5 MΩ. Care was taken to seal patch pipettes gently in control and *mdx* cells; usually, on contact of the pipette with the cell, the release of positive pressure from the pipette was sufficient to form a gigaseal.

Solutions and Chemicals. Pipettes were filled with Tyrode's solution containing (in mM) 140 NaCl, 5 KCl, 2.5 $CaCl_2$, 1 $MgCl_2$, and 10 Hepes adjusted to pH 7.4 with NaOH. In cell-attached experiments, fibers were bathed in external K^+-rich solution containing (in mM) 140 KCl, 2.5 $CaCl_2$, 1 $MgCl_2$, and 10 Hepes adjusted to pH 7.4 with KOH. For inside-out experiments, calibration solutions were used to control the free [Ca^{2+}] at the cytoplasmic face of membrane patches. Calibration solutions were prepared from two stock solutions containing (in mM)

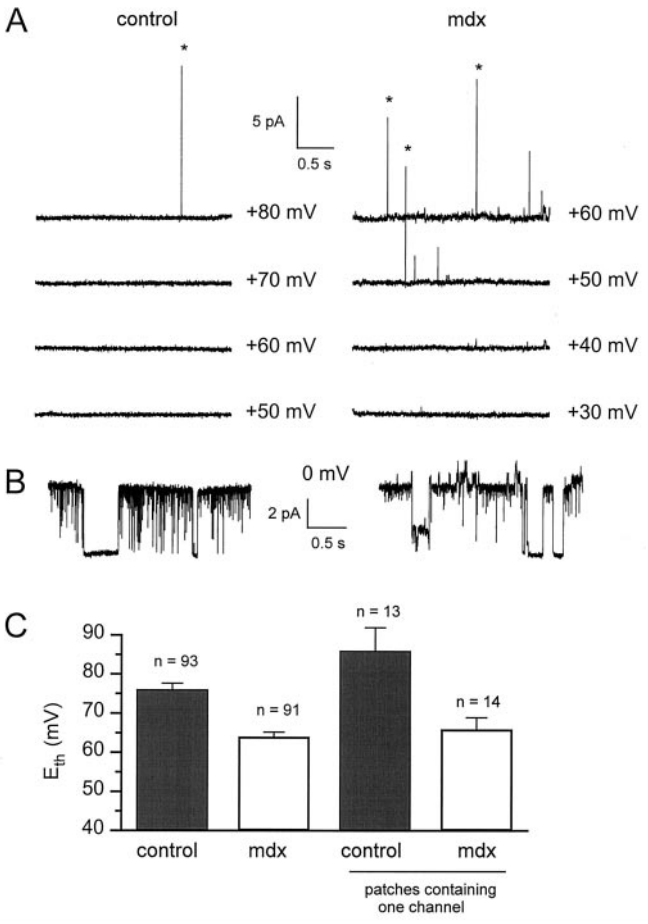

Fig. 3. Measurement of E_{th} in cell-attached patches from control and *mdx* muscle fibers. (*A*) Segments of current traces obtained in response to voltage pulses given at values indicated next to each trace from a holding potential of 0 mV. Asterisks indicate opening of K_{Ca} channels. (*B*) Segments of current traces obtained from the same patches shown in *A* after excision in the 2.5 mM Ca^{2+}-containing bath solution. (*C*) Comparison of E_{th} in control and *mdx* cell-attached patches.

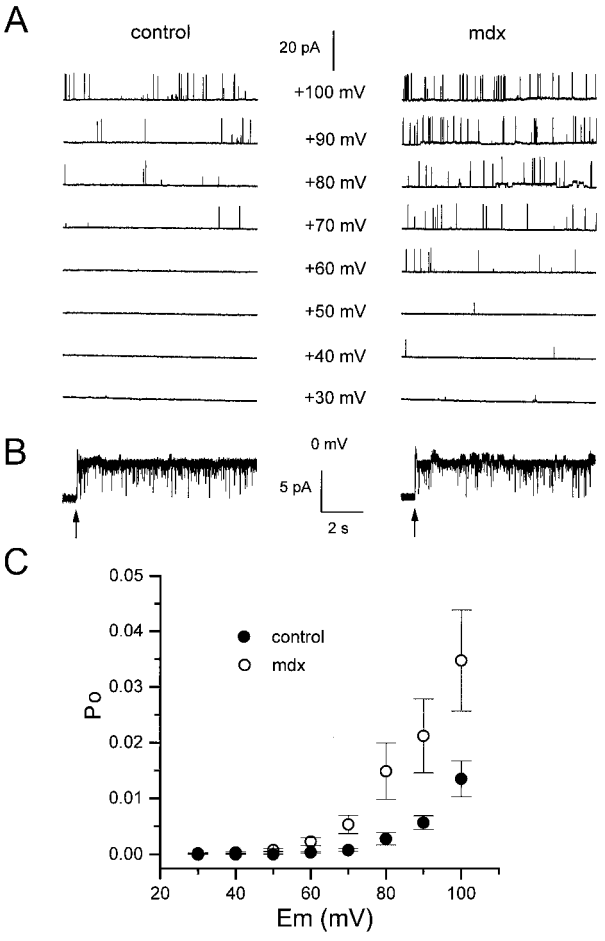

Fig. 4. Voltage activation properties of K_{Ca} channels in cell-attached patches from control and *mdx* muscle fibers. (*A*) Segments of current traces obtained in response to voltage pulses given at values indicated next to each trace from a holding potential of 0 mV. (*B*) Segments of current traces obtained from the same patches shown in *A* after excision (indicated by arrows) in the 2.5 mM Ca^{2+}-containing bath solution. (*C*) Relationships between P_o and membrane potential in 35 control (●) and 39 *mdx* (○) cell-attached patches.

100 KCl, 10 EGTA, 10 Pipes at pH 7.2 with and without 10 $CaCl_2$. Various free [Ca^{2+}] were achieved by mixing these two stock solutions in different ratios. Membrane patches were exposed to different solutions by placing them in the mouth of a perfusion tube from which flowed the rapidly exchanged solutions.

Statistics. Nonlinear least-squares fits were performed with a Marquardt–Levenberg algorithm routine included in MICROCAL ORIGIN (Microcal Software, Northampton, MA). Data values are presented as means ± SEM. Data were analyzed statistically with Student's unpaired *t* test. Values were considered significant when $P < 0.05$.

Results

Comparison of Ca^{2+} and Voltage Sensitivity of K_{Ca} Channels in Control and *mdx* Muscle Fibers. Before using K_{Ca} channels as submembranous Ca^{2+} probe, a first set of experiments was performed by using the inside-out configuration to determine whether the main characteristics of K_{Ca} channels, i.e., Ca^{2+}- and voltage-sensitivity, were modified in *mdx* muscle fibers. Fig. 1 illustrates the Ca^{2+}-dependence properties of K_{Ca} channels in inside-out patches from control (Fig. 1 *Left*) and *mdx* muscle fibers (Fig. 1 *Right*). In these experiments, membrane patches were clamped at 0 mV and exposed in a cumulative manner to internal solutions containing increasing concentrations of free Ca^{2+}. In the presence of 1.7 μM calcium at the cytoplasmic face, opening of channels that correspond to ATP-dependent K^+ channels, as described in a previous study with similar experimental conditions (28, 29), were detected both in control and *mdx* muscle fibers. At 3 μM Ca^{2+}, K_{Ca} began to open, and on increasing free Ca^{2+} concentrations, K_{Ca} channel gradually activated in both muscle types; in the presence of 4.4, 8.4, 14, and 30 μM Ca^{2+}, P_o was 0.07, 0.63, 0.8, and 0.9 in the control patch, respectively, compared with 0.07, 0.34, 0.7 and 0.9 in the *mdx* patch, respectively. Fig. 1*B* shows the dose dependence of activation of K_{Ca} channels versus [Ca^{2+}] in control and *mdx* muscle fibers. In each patch, experimental data were fitted by a Hill equation: $P_o = [Ca^{2+}]^n/([Ca^{2+}]^n + K^n)$, where K is the [Ca^{2+}] at which activation is half-maximal and n is the slope factor (Hill coefficient). The mean values for n and K were 4.5 ± 0.4 and 6.9 ± 0.8 μM in 14 control patches compared with 4.5 ± 0.7 and 7.7 ± 0.55 μM in 19 *mdx* patches, respectively. These values were not significantly different ($P = 1$ and 0.4, respectively).

Comparison of voltage-dependence of K_{Ca} channels in control and *mdx* muscle fibers was done by applying membrane depolarization of increasing amplitude to inside-out patches exposed to an internal solution containing 4.4 μM Ca^{2+} (Fig. 2). On

depolarizing the patch, channel opening increased, and at −30, −10, +10, +30, and +50 mV, P_o was 0.32, 0.6, 0.85, 0.96, and 0.98, respectively, in the control patch, compared with 0.24, 0.5, 0.87, 0.96, and 0.98, respectively, in the *mdx* patch. Fig. 2*B* shows the relationship between P_o of K_{Ca} channels and membrane potential in patches from control and *mdx* muscle fibers. In each patch, experimental data were fitted by a Boltzman equation [$P_o = 1/(1 + e^{(V_{1/2} - V)/k})$]. The mean values for $V_{1/2}$ and k were 12.3 ± 5.4 mV and 11.5 ± 0.7 mV in 14 control patches compared with 13 ± 4 mV and 12 ± 0.9 mV in 16 *mdx* patches, respectively. These values were not significantly different ($P = 0.99$ in both cases).

Finally, the amplitude of unitary current through K_{Ca} channels was plotted against membrane potential in control and *mdx* inside-out patches under the same ionic conditions described above (Fig. 2*C*). It can be seen that the current-voltage relationship obtained in *mdx* patches is superimposed on the one obtained in control patches. The mean conductance at 0 mV was 68 pS.

On the basis of these results, it can be concluded that the conductance and Ca^{2+} and voltage sensitivity of K_{Ca} channels are similar in control and *mdx* skeletal muscle fibers.

Voltage Activation of K_{Ca} Channels in Control and *Mdx* Cell-Attached Patches. Because K_{Ca} channels had the same properties in control and *mdx* muscle, we took advantage of the Ca^{2+}-sensitivity of these K^+ channels to probe the subsarcolemmal Ca^{2+} in control and *mdx* muscle fibers. The subsarcolemmal [Ca^{2+}] was compared in control and *mdx* muscle fibers by measuring E_{th} in cell-attached patches, i.e., the membrane voltage at which a first K_{Ca} opening was detected. Any difference in E_{th} between control and *mdx* muscle fibers should indicate a difference in the subsarcolemmal [Ca^{2+}] in these cell types. During these experiments, the procedure described in Fig. 3 was used. Cell-attached patches were established on control and *mdx* muscle fibers bathed in K^+-rich solution to clamp the cell internal potential close to 0 mV. The membrane potential was brought to increasing depolarized levels from a holding potential of 0 mV by voltage steps of 10-mV amplitude until an opening of K_{Ca} channels was detected. In the control cell-attached patch illustrated in Fig. 3*A Left*, E_{th} was found at +80 mV. Indeed, a first opening of a channel carrying an outward current of 15 pA and then identified as a K_{Ca} channel on the basis of its high conductance (90 pS at +80 mV) was observed at +80 mV (Fig. 3*A*). Subsequent excision and exposition of the patch to the 2.5 mM Ca^{2+}-containing bath solution revealed that one K_{Ca} channel was present in this patch (Fig. 3*B Left*).

A typical result obtained in an *mdx* cell-attached patch with the same protocol is illustrated in Fig. 3*A Right*. In this patch, E_{th} was found at +50 mV. Subsequent excision of the patch indicated that one K_{Ca} channel was present in this patch too (Fig. 3*B Right*).

Fig. 3*C* shows that, in 93 control cell-attached patches, mean E_{th} was +76 ± 1.6 mV compared with +64 ± 1.2 mV in 91 *mdx* patches, a value significantly lower ($P < 0.001$). However, E_{th} relies on the number of channels in the patch; E_{th} was then compared in cell-attached patches containing one channel. In these one-channel-containing patches, E_{th} was +86 ± 6 mV in 13 control cell-attached patches compared with +66 ± 3 mV in 14 *mdx* cell-attached patches. These values were significantly different ($P = 0.0054$).

The above results suggest that the voltage activation curve of K_{Ca} channels in *mdx* cell-attached patches may be shifted toward less positive membrane potentials. To confirm this tendency, the voltage activation curve of K_{Ca} channels was built in control and *mdx* cell-attached patches (Fig. 4). The same experimental protocol described above was used except that voltage pulses lasted 10 s. Fig. 4*A* illustrates results obtained in a control and in an *mdx* cell-attached patch. In the control patch, E_{th} was +70 mV, and in the *mdx* patch, E_{th} was +40 mV. As depolarization increased, P_o augmented in both patches but with a lower value for a given potential in the control compared with the *mdx* patch. In the control patch, P_o was 0.001, 0.0005, 0.0034, and 0.016 at +70, +80, +90, and +100 mV, respectively. In the *mdx* patch, P_o was 0.002, 0.007, 0.01, 0.02, and 0.036 at +60, +70, +80, +90, and +100 mV, respectively. Excision revealed that the two patches contained one channel (Fig. 4*B*). Fig. 4*C* shows the voltage activation curve of K_{Ca} channels obtained in 35 control and 39 *mdx* cell-attached patches up to +100 mV, the highest membrane potential that could be maintained under these experimental conditions. In accordance with the shift in E_{th} between control and *mdx* patches described above, it can be observed that the voltage activation curve tended to be shifted by also 20 mV toward less positive potentials for *mdx* patches. Statistical analysis indicated that the mean P_o was significantly lower in control than in *mdx* cell-attached patches at +60, +70, +80, +90, and +100 mV (P was 0.01, 0.008, 0.025, 0.014, and 0.022, respectively).

Estimation of the Difference in Subsarcolemmal [Ca^{2+}] Between Control and *mdx* Muscle Fibers. A shift in E_{th} to lower membrane potential in cell-attached patches from *mdx* muscle fibers suggests that the subsarcolemmal [Ca^{2+}] is higher in *mdx* muscle. In an attempt to estimate the magnitude of the increase in [Ca^{2+}] at the submembranous level in *mdx* muscle, we determined, in inside-out patches, the shift in the [Ca^{2+}] that has to be imposed at the cytoplasmic face to produce a 20-mV shift in the threshold.

In these experiments, inside-out patches were excised from control muscle fibers and exposed to internal solutions containing increasing concentrations of free Ca^{2+} of 20, 30, 70, 100, 300, and 700 nM. These [Ca^{2+}] were chosen in respect to their ability to trigger the first opening of K_{Ca} channels at membrane potentials close to E_{th} values obtained in cell-attached patches (i.e., between +40 and +90 mV). In the presence of each free Ca^{2+} concentration, the same pulse protocol as the one applied in cell-attached patches was used to determine E_{th} (Fig. 5). At 30 nM Ca^{2+}, only ATP-dependent K^+ channels were active, and no K_{Ca} channel opening was observed up to +80 mV. The first opening of K_{Ca} channels was observed at +80, +70, and +50 mV in the presence of 100, 300, and 700 nM Ca^{2+}, respectively. In each patch where this protocol was applied, E_{th} was plotted as a function of [Ca^{2+}] (Fig. 5*B*). A linear regression was adjusted to each relationship between E_{th} and the logarithm of [Ca^{2+}] as described by Moczydlovski and Latorre (30) for the voltage dependence of Ca^{2+} dissociation constants of K_{Ca} channels incorporated into planar lipid bilayers. In 22 patches, the mean slope was −38.65 ± 3.35, indicating that a decrease of 20 mV in the E_{th} implies a 3.3-fold increase in the [Ca^{2+}] at the cytoplasmic face. Of these 22 patches, in the 6 patches containing one channel, the mean slope and constant value of the linear relationship between E_{th} and logarithm of [Ca^{2+}] were −42.8 ± 5.8 and 154 ± 16, respectively (Fig. 5*C*). With these parameters, a shift in E_{th} from +86 mV to +66 mV (the shift in E_{th} observed between control and *mdx* cell-attached patches) yielded an increase in [Ca^{2+}] from 40 to 115 nM.

Discussion

In this study, we show that E_{th} is significantly lower in *mdx* muscle fibers. Because the properties of K_{Ca} channels in terms of Ca^{2+} and voltage dependence were found to be the same in control and *mdx* muscle fibers, this result suggests that the subsarcolemmal [Ca^{2+}] is higher in *mdx* than in normal skeletal muscle fibers. Our inside-out experiments indicated that the 20-mV lower E_{th} in *mdx* muscle might correspond to a ≈3-fold increase in the subsarcolemmal [Ca^{2+}]. The subsarcolemmal [Ca^{2+}] was then estimated at 40 nM in control versus 115 nM in *mdx* muscle fibers. We are aware that these estimations are based on the assumption that K_{Ca} channels have the same behavior in inside-

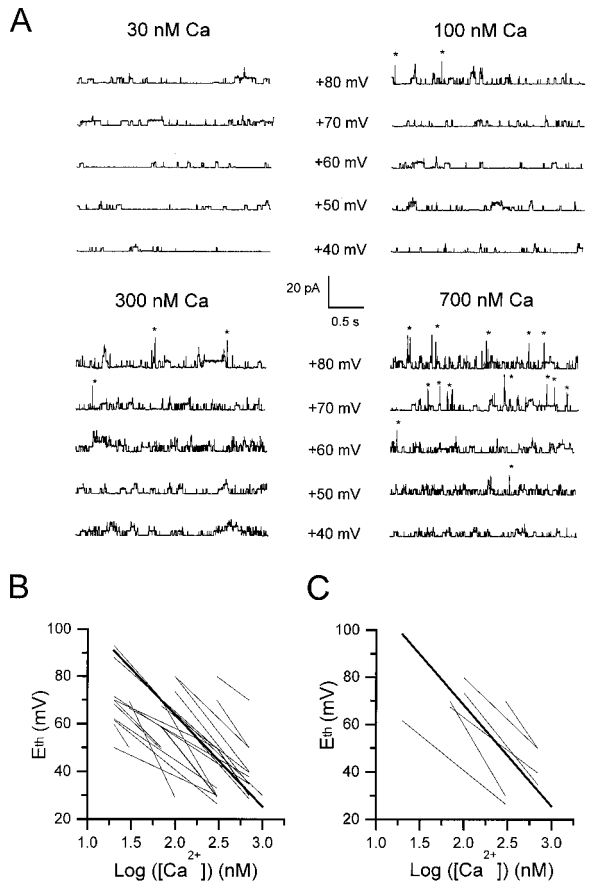

Fig. 5. Measurement of E_{th} in inside-out patches from control muscle fibers in the presence of increasing concentrations of intracellular free Ca^{2+}. (*A*) Segments of current traces obtained in response to voltage pulses given at values indicated next to each trace from a holding potential of 0 mV in the presence of 30, 100, 300, and 700 nM Ca^{2+}. Asterisks indicate opening of K_{Ca} channels. (*B*) Whole set of linear fits between E_{th} and logarithm of $[Ca^{2+}]$ in 22 patches (thin lines); the bold line corresponds to the mean fit with a slope of −38.65 (see text), which has been arbitrarily positioned on the graph; data points are not shown for clarity. (*C*) Whole set of linear fits between E_{th} and logarithm of $[Ca^{2+}]$ in six one-channel containing patches (thin lines); the bold line corresponds to the mean fit with a slope of −42.8 and a constant value of 154 (see text); data points are not shown for clarity.

out and cell-attached patches. We cannot exclude that, *in situ*, the presence of intracellular factors such as Mg^{2+} or associated cytoplasmic proteins may modify the Ca^{2+} and/or voltage-sensitivity of K_{Ca} channels (31, 32). Along this line, Muñoz *et al.* (33), combining microfluorometry and single-channel recording in smooth muscle cells, showed that K_{Ca} channels had a higher cooperativity for activation by Ca^{2+} in intact cells than in excised patches. Estimated absolute values of subsarcolemmal $[Ca^{2+}]$ thus have to be taken with caution, but we can expect that the relative 3-fold increase in $[Ca^{2+}]$ yielding to a 20-mV displacement of E_{th} in excised patches actually corresponds to the relative increase in subsarcolemmal $[Ca^{2+}]$ in *mdx* muscle fibers.

Our finding favors the hypothesis according to which an increased calcium entry is associated with the absence of dystrophin in *mdx* skeletal muscle. It has indeed been shown that leak or stretch-regulated calcium channels had a significant higher open probability in cultured myotubes and adult muscle fibers from *mdx* mice (9, 34); more recently, using a manganese quench technique, Tutdibi *et al.* (14) reported that the membrane permeability to divalent cations in *mdx* fibers was twice the value of controls. However, the relevant question was whether this elevated sarcolemmal Ca^{2+} influx in dystrophic muscle gave rise to an augmentation in the intracellular $[Ca^{2+}]$. In a recent study, using indo-1 fluorescence methods, Collet *et al.* (15) failed to detect any drastic change in the resting intracellular $[Ca^{2+}]$ as well as in depolarization-induced Ca^{2+} transients under voltage control in *mdx* muscle fibers. Our present finding might indicate that a Ca^{2+} overload does exist in *mdx* muscle but is restricted to the subsarcolemmal compartment. There is now evidence that intracellular Ca^{2+} gradients exist between the subsarcolemmal space and the cytosolic bulk in different cell types. In a number of studies, these Ca^{2+} microdomains have also been monitored by Ca^{2+} activation of plasmalemmal K^+ channels. They are thought to rise at the point of Ca^{2+} entry, for instance, through nicotinic receptors at the endplate of skeletal muscle (28), through voltage-dependent calcium channels in neurons (35) or/and at the site of Ca^{2+} release from sarcoplasmic reticulum in smooth and skeletal muscles (19, 36). However, in the aforementioned processes, the increase in submembranous $[Ca^{2+}]$ was transient, whereas our results suggest that a permanent flux of calcium overloads the subsarcolemmal compartment in *mdx* muscle. It must then be assumed that the influx of calcium might overcome the local Ca^{2+}-sequestering mechanisms in *mdx* muscle.

A restricted elevated $[Ca^{2+}]$ at the subsarcolemmal level in *mdx* muscle has physiopathological relevance. It has been shown that μ-calpain, a Ca^{2+}-activated protease, has an increased activity in *mdx* muscle, suggesting a role of this protease in the degenerative aspects of the disease (37). Interestingly, it has also been proposed that calpain activation requires the association of the protease with the cell membrane (38) at the level of which phospholipids act as calpain activators (39, 40). Activator proteins of calpain have also been identified and are also thought to function attached to the plasma membrane (41, 42). Taken together, these data suggest that calpain activity is potentiated at the submembranous level. Accumulation of Ca^{2+} near the membrane of *mdx* muscle fibers could then reinforce calpain activation at this strategic location and trigger necrotic events. Because calpain was shown to increase the activity of Ca^{2+} leak channels (43) and decrease the activity of Ca^{2+}-ATPases (44), one can speculate that the degenerative process *mdx* skeletal muscle cells undergo results from a chain of the following events: increased Ca^{2+} influx, accumulation of Ca^{2+} under the membrane, activation of protease, further increase in Ca^{2+} influx, and so on.

We are grateful to Oger Rougier for helpful discussion while the manuscript was in preparation. This study was supported by funds from the Centre National de la Recherche Scientifique, the Université Claude Bernard Lyon 1, and the Association Française Contre les Myopathies (to A.F.M.).

1. Hoffman, E. & Kunkel, L. M. (1989) *Neuron* **2,** 1019–1029.
2. Matsumara, K. & Campbell, K. P. (1994) *Muscle Nerve* **17,** 2–15.
3. Straub, V. & Campbell, K. P. (1997) *Curr. Opin. Neurol.* **10,** 168–175.
4. Bulfield, G., Siller, W. G., Wight, P. A. & Moore, K. J. (1984) *Proc. Natl. Acad. Sci. USA* **81,** 1189–1192.
5. Franco, A., Jr., & Lansman, J. B. (1990) *Nature (London)* **344,** 670–673.
6. Haws, C. M. & Lansman, J. B. (1991) *Proc. R. Soc. London Ser. B* **245,** 173–177.
7. Fong, P., Turner, P. R., Denetclaw, W. F. & Steinhardt, R. A. (1990) *Science* **250,** 673–676.
8. Turner, P. R., Fong, P., Denetclaw, W. F. & Steinhardt, R. A. (1991) *J. Cell Biol.* **115,** 1701–1712.
9. Hopf, F. W., Turner, P. R., Denetclaw, W. F., Reddy, P. & Steinhardt, R. A. (1996) *Am. J. Physiol.* **271,** C1325–C1339.
10. Turner, P. R., Westwood, T., Regen, C. M. & Steinhardt, R. A. (1988) *Nature (London)* **335,** 735–738.
11. Head, S. I. (1993) *J. Physiol. (London)* **469,** 11–19.
12. Gailly, P., Boland, B., Himpens, B., Casteels, R. & Gillis, J. M. (1993) *Cell Calcium* **14,** 473–483.
13. Pressmar, J., Brinkmeier, H., Seewald, M. J., Naumann, T. & Rüdel, R. (1994) *Pflügers Arch.* **426,** 499–505.
14. Tutdibi, O., Brinkmeier, H., Rüdel, R. & Föhr, K. J. (1999) *J. Physiol. (London)* **515,** 859–868.

15. Collet, C., Allard, B., Tourneur, Y. & Jacquemond, V. (1999) *J. Physiol. (London)* **520,** 417–429.
16. Gillis, J. M. (1996) *Acta Physiol. Scand.* **156,** 397–406.
17. Bruton, J. D., Katz, A. & Westerblad, H. (1999) *Proc. Natl. Acad. Sci. USA* **96,** 3281–3286.
18. Etter, E. F., Minta, A., Poeni, M. & Fay, F. S. (1996) *Proc. Natl. Acad. Sci. USA* **93,** 5368–5373.
19. Ganitkevich, V. Y. & Isenberg, G. (1996) *J. Physiol. (London)* **490,** 305–318.
20. Blatz, A. L. & Magleby, K. L. (1987) *Trends Neurosci.* **10,** 463–467.
21. Latorre, R., Oberhauser, A., Labarca, P. & Alvarez, O. (1989) *Annu. Rev. Physiol.* **51,** 385–399.
22. McManus, O. B. (1991) *J. Bioenerg. Biomembr.* **23,** 537–559.
23. Kaczorowski, G. J., Knaus, H.-G., Leonard, R. J., McManus, O. B. & Garcia, M. L. (1996) *J. Bioenerg. Biomembr.* **28,** 255–267.
24. Vergara, C., Latorre, R., Marrion, N. V. & Adelman, J. P. (1998) *Curr. Opin. Neurobiol.* **8,** 321–329.
25. Hocherman, S. D. & Bezanilla, F. (1996) *J. Physiol. (London)* **493,** 113–128.
26. DiMario, J. X., Uzman, A. & Strohman, R. C. (1991) *Dev. Biol.* **148,** 314–321.
27. Berthier, C., Amsellem, J. & Blaineau, S. (1995) *J. Muscle Res. Cell Motil.* **16,** 553–566.
28. Allard, B., Bernengo, J.-C., Rougier, O. & Jacquemond, V. (1996) *J. Physiol. (London)* **494,** 337–349.
29. Allard, B. & Rougier, O. (1997) *J. Physiol. (London)* **498,** 319–325.
30. Moczydlovski, E. & Latorre, R. (1983) *J. Gen. Physiol.* **82,** 511–542.
31. Golowasch, J., Kirkwood, A. & Miller, C. (1986) *J. Exp. Biol.* **124,** 5–13.
32. Schopperle, W. M., Holmqvist, M. H., Zhou, Y., Wang, J., Wang, Z., Griffith, L. C., Keselman, I., Kusinitz, F., Dagan, D. & Levitan, I. B. (1998) *Neuron* **20,** 565–573.
33. Muñoz, A., Garcia, L. & Guerrero-Hernandez, A. (1998) *Biophys. J.* **75,** 1774–1782.
34. Franco-Obregon, A. & Lansman, J. B. (1994) *J. Physiol. (London)* **481,** 299–309.
35. Marrion, N. V. & Tavalin, S. J. (1998) *Nature (London)* **395,** 900–905.
36. Jacquemond, V. & Allard, B. (1998) *J. Physiol. (London)* **509,** 93–102.
37. Spencer, M. J., Croall, D. E. & Tidball, J. G. (1995) *J. Biol. Chem.* **270,** 10909–10914.
38. Molinari, M., Anagli, J. & Carafoli, E. (1994) *J. Biol. Chem.* **269,** 27992–27995.
39. Saido, T. C., Shibata, M., Takenawa, T., Murofushi, H. & Suzuki, K. (1992) *J. Biol. Chem.* **267,** 24585–24590.
40. Arthur, J. S. C. & Crawford, C. (1996) *Biochim. Biophys. Acta* **1293,** 201–206.
41. Melloni, E., Michetti, M., Salamino, F., Sparatore, B. & Pontremoli, S. (1998) *Biochem. Biophys. Res. Commun.* **249,** 583–588.
42. Michetti, M., Viotti, P. L., Melloni, E. & Pontremoli, S. (1991) *Eur. J. Biochem.* **202,** 1177–1180.
43. Turner, P. R., Schultz, R., Ganguly, B. & Steinhardt, R. A. (1993) *J. Membr. Biol.* **133,** 243–251.
44. Salamino, F., Sparatore, B., Melloni, E., Michetti, M., Viotti, P. L., Pontremoli, S. & Carafoli, E. (1994) *Cell Calcium* **15,** 28–35.